CO_2 hydrogenation to hydrocarbons over Co and Fe-based Fischer-Tropsch catalysts

*Carlo Giorgio Visconti *, Michela Martinelli, Leonardo Falbo, Laura Fratalocchi, Luca Lietti **

Politecnico di Milano, Dipartimento di Energia, via La Masa, 34–20156 Milano, Italy

A B S T R A C T

The performances of representative Co-based and Fe-based Fischer-Tropsch catalysts have been comparatively investigated in the hydrogenation of CO and CO_2. Over an un-promoted Co/γ-Al_2O_3 catalyst, CO_2 is easily hydrogenated and its conversion rate is even faster than that of CO; however, the selectivities of the two processes are extremely different, with methane largely dominating the product distribution in the case of CO_2 hydrogenation and long-chain hydrocarbons dominating the products pool during CO hydrogenation. As opposite to cobalt, CO_2 hydrogenation rate over K-promoted 100Fe/10Zn/1Cu (at/at) catalysts is slower than that of CO, but the products are dominated by middle distillates when CO_2 replaces CO in the feed. Such behaviors depend on the different adsorption strengths of CO and CO_2, which affect the H/C atomic ratio on the catalyst surface. In the case of Fe-based catalyst, we have also found that the catalytic sites active in the chain growth process (iron carbides) are transformed into sites active in the hydrogenation reactions (iron oxides/reduced iron centers) at low CO partial pressures. Potassium has a key role in promoting the stability of chain growth sites, thus decreasing the secondary reactions of olefins.

Keywords:
CO_2 hydrogenation
Iron catalyst
Cobalt catalyst
Fischer-Tropsch synthesis
Potassium

1. Introduction

The reduction of CO_2 emissions into the atmosphere has become an important research topic in recent years because carbon dioxide is one of the major contributors to the green-house effect, and its worldwide production is growing [1,2].

A first strategy to reduce CO_2 emissions, which has been deeply investigated in the last years and which has been recently applied for the first time to a large-scale power station in Canada [3], is Carbon Capture and Storage (CCS) [4], which consists in the permanent CO_2 storage deep underground in very specific geological sites. A very attractive alternative to this technology is represented by Carbon Capture and Utilization (CCU) processes, which consist in the chemical conversion of CO_2 to added-value carbon-containing products. Among them, the large-scale conversion of CO_2 into liquid fuels is of great interest, because the broad market of these products would guarantee an appreciable decrease of the global CO_2 emissions, limiting at the same time the consumption of fossil fuels.

A R T I C L E I N F O

Article history:
Received 13 January 2016
Received in revised form 14 March 2016
Accepted 6 April 2016
Available online 3 May 2016

In principle, carbon dioxide may be hydrogenated to liquid fuels either by direct or indirect routes. In the indirect route, CO_2 is converted to methanol, which can be then transformed into hydrocarbons through the commercially available methanol-to-gasoline (MTG) process based on zeolite catalysts [5]. On the contrary, in the direct route, CO_2 is converted to fuels through a modified Fischer-Tropsch (FT) process, eventually followed by a product upgrading (hydrotreating) step [2,6–29]. In this work we have focused on this latter alternative.

Literature data show that both CO and CO_2 can be hydrogenated over both cobalt [5–9,25–29] and iron [2,6,9,12–25] FT catalysts; however, most of the authors found that the product distribution during CO and CO_2 hydrogenation are very different. Indeed, CO_2 hydrogenation leads mainly to light saturated hydrocarbons with lower chain growth probability (α) values if compared to CO hydrogenation.

On cobalt-based catalysts, which are known to be substantially inactive in the water-gas-shift (WGS) and in the reverse-water-gas-shift (RWGS) processes, the reason of the different reactivity of CO and CO_2 is still debated. Moreover, the catalyst stability in the presence of CO_2 is still unclear and scarce experimental data are available to date. Zhang et al. [10] propose two different reaction pathways, with CO hydrogenation going through HC* and *OH ad-

* Corresponding authors.
E-mail addresses: carlo.visconti@polimi.it (C.G. Visconti), luca.lietti@polimi.it (L. Lietti).

Published Journal Article available at: http://dx.doi.org/10.1016/j.cattod.2016.04.010

Table 1
Metal loading and textual properties of Fe and Co catalysts.

	Metalloading[wt.%]	Surface area[m^2/g]	Pore volume[cm^3/g]	Average porediameter[Å]
Fe2K	61.9	76	0.21	90
Fe4K	61.0	114	0.25	66
Fe10K	58.4	102	0.21	63
Co/γ-Al_2O_3	15.0	120	0.31	85

species and CO_2 hydrogenation involving the HC*O intermediate, eventually leading to methane. As opposite, Visconti et al. [8] propose the same mechanism for CO and CO_2 hydrogenation processes, but ascribe the change in the product distribution to the different hydrogen to carbon ratio on the catalyst surface during the two processes. In the case of CO_2 hydrogenation, a higher H/C surface ratio would be obtained as a consequence of the weak CO_2 adsorption strength, which would favour the hydrogenation of the adsorbed C-containing surface intermediates, thus bringing to a decrease of the chain growth probability. Similarly to Visconti et al. [8], Riedel et al. [7] attribute the change in the product composition when switching from CO to CO_2 to the loss of "selective inhibition" which dominates the FT regime. Indeed, according to these authors, during CO hydrogenation, high CO partial pressure and strong CO adsorption result in a low concentration of H-adspecies. This slows down CH_3* hydrogenation to methane and secondary olefins hydrogenation to the corresponding paraffins, thus resulting in the high values of the chain growth probability typical of FT regime. The same does not happen during CO_2 hydrogenation, when both the low adsorption strength of CO_2 and the low CO partial pressure are insufficient to inhibit H_2 adsorption, thus bringing to low molecular weight saturated hydrocarbons.

On iron based catalysts, which are usually preferred to convert CO_2 to heavy hydrocarbons because of their intrinsic activity in the RWGS reaction [2,30], researchers agree that CO_2 hydrogenation pathway involves CO as intermediate [18] and the different H_2/CO ratio in the reactor during CO and CO_2 hydrogenation is considered the major reason for the different selectivity of the two processes [13,14,19]. Indeed, the H_2/CO ratio is reported to affect both the process kinetics [13,14,19] and the nature of the active sites [21]. However, as in the case of Co-based catalysts, only few information are available on the catalyst stability when CO_2 replaced CO in the feed.

The reactivity of CO_2 on Co- and Fe-based catalysts in the presence of CO is also a matter of discussion in the literature. Indeed, even if almost all the literature papers available so far report that CO_2 can be effectively hydrogenated only at low partial pressure of CO (e.g., [8,14]), different evidences have been reported on the effect of the presence of CO_2 on the CO conversion rate as well as on the product distribution. Chun et al. [31], for example, observe an inhibiting effect of CO_2 in terms of hydrocarbon yield, but also report that the product distribution is not affected by the presence of CO_2, as well as the olefin to paraffin (O/P) ratio in the hydrocarbon products. They attribute such effects to a competitive adsorption of CO and CO_2. As opposite to these results, other authors [20] have found that both CO conversion rate and product distribution are not affected by the presence of CO_2.

Given these premises, it is clear that further efforts to clarify the reactivity of Co and Fe Fischer-Tropsch catalysts in the presence of CO_2 and CO/CO_2 mixtures are needed. Accordingly, the first aim of this work is the cross-comparison between CO and CO_2 hydrogenation processes carried out for more than 400 h on representative iron and cobalt based FT catalysts. To the scope, both the CO_x conversion and the product distribution have been measured on two state-of-the-art catalysts under transient and steady-state conditions. A particular attention has been devoted to the quantification of paraffins and olefins in the products, because their relative content can give informative indications on the nature of active sites.

In the second part of the work, the effect of alkali loading (K/Fe atomic ratio between 0.02 and 0.1) on a state-of-the-art Fe/Zn/Cu/K catalyst has been investigated. Indeed, it is expected that potassium, by donating electrons to iron, could affect the catalyst selectivity by changing the adsorption strength of reactants and products on the active sites. Such effect, which has been largely investigated during CO hydrogenation [32–35], has been only scarcely studied during CO_2 or CO/CO_2 mixtures hydrogenation [13,17,19,22,24].

2. Experimental

2.1. Catalysts preparation

2.1.1. Fe-based catalysts

Following the procedure reported in [32], a 100Fe/10Zn precursor (atomic ratios) was prepared via semi-batch co-precipitation of iron(III) and zinc nitrates at constant pH to form porous Fe-Zn oxy/hydroxycarbonates powder. Briefly, an aqueous solution containing $Fe(NO_3)_3{\cdot}9H_2O$ (3.0 M) was mixed with an aqueous solution of $Zn(NO_3)_2{\cdot}6H_2O$ (1.4 M). The resulting solution was slowly introduced in a jacketed quartz reaction cell kept at 80 °C, containing a buffer aqueous solution ($(NH_4)_2CO_3$ 1.0 M) acidified at pH of 7. A solution of $(NH_4)_2CO_3$ 1.0 M was also added to the cell by keeping the pH of the slurry at a value of 7 ± 0.2. The obtained slurry was filtered and the solid was washed with deionized water (further details can be found in Ref. [20]). The sample was eventually dried in static air at 120 °C overnight and the resulting powders were calcined in stagnant ambient air at 350 °C for 1 h (heating rate 1 °C/min). Obtained powder was promoted by incipient wetness impregnation with potassium carbonate and copper nitrate aqueous solutions, dried at 120 °C overnight and calcined at 400 °C for 4 h [20]. Samples with a Cu/Fe atomic ratio of 0.01 and K/Fe atomic ratios of 0.02, 0.04 and 0.1 were prepared, indicated in the following as "Fe2K" (100Fe/10Zn/1Cu/2 K), "Fe4K" (100Fe/10Zn/1Cu/4 K) and "Fe10K" (100Fe/10Zn/1Cu/10 K), respectively.

2.1.2. Co-based catalysts

The 15 wt.% Co/γ-Al_2O_3 catalyst used in this study (sample tag "Co/γ-Al_2O_3") was a bench-scale prepared sample obtained by incipient wetness impregnation of γ-Al_2O_3 with a cobalt nitrate hexahydrate aqueous solution. Details of the preparation procedure can be found in Ref. [8].

2.2. Catalyst characterization and testing

The morphological properties (BET area, BJH pore volume and average pore size) of the different catalysts, determined by nitrogen adsorption-desorption at 77 K using Micromeritics TriStar 3000 instrument, are reported in Table 1.

Activity tests of Fe-based and Co/γ-Al_2O_3 catalysts were carried out in two separate lab-scale rigs and at different process conditions (Tables 2 and 3), similar to those adopted at the industrial scale for the Fischer-Tropsch synthesis. Those rigs are described in the

Table 2
Process conditions adopted in CO_2, CO and CO/CO_2 hydrogenation tests for Fe-based catalysts.

Condition number	#1	#2	# 3
Condition tag	$CO_2/H_2/N_2$	$CO/H_2/N_2$	$CO/H_2/CO_2$
T [°C]	220	220	220
GHSV [$cm^3(STP)h^{-1}g_{cat}^{-1}$]	6000	6000	6000
P [barg]	30	30	30
P^0_{H2} [barg]	9.6	9.6	9.6
P^0_{CO} [barg]	–	9.6	9.6
P^0_{CO2} [barg]	9.6	–	9.6
P^0_{N2} [barg]	10.8	10.8	–
P^0_{Ar} [barg]	–	–	1.2

Table 3
Process conditions adopted in CO and CO_2 hydrogenation tests for $Co/\gamma\text{-}Al_2O_3$ catalyst.

Condition number	#1	#2
Condition tag	H_2/CO	H_2/CO_2
T [°C]	220	220
GHSV [$cm^3(STP)h^{-1}g_{cat}^{-1}$]	4800	4800
P [barg]	20	20
P^0_{H2} [barg]	14.20	14.20
P^0_{CO} [barg]	5.68	–
P^0_{CO2} [barg]	–	5.68
P^0_{Ar} [barg]	0.12	0.12

following. Carbon selectivity to the *i* species (S_i) has been calculated according to the following equation:

$$S_i = \frac{F_i^{OUT} \cdot n_i}{F_{CO}^{IN} \cdot \chi_{CO} + F_{CO_2}^{IN} \cdot \chi_{CO_2}}$$

Where F_i^{OUT} is the molar productivity of *i* species, n_i is the carbon number of this species, F_{CO}^{IN} is the CO inlet molar flow, χ_{CO} is the CO conversion, $F_{CO_2}^{IN}$ is the CO_2 inlet molar flow, and χ_{CO_2} is the CO_2 conversion.

2.2.1. Fe-based catalysts

Tests with Fe-based catalysts were carried out in a high-pressure lab-scale plant, operated 24/7, equipped with a stainless steel fixed-bed reactor (I.D. = 1.1 cm, length = 85 cm), placed into a vertical electric furnace. More details on the experimental rig and on the adopted process analytics can be found elsewhere [20]. We recall here that the adopted set-up allowed us to quantify the composition of the C_1–C_{10} hydrocarbon fraction, in addition to CO, CO_2, H_2, N_2, Ar.

Prior to the activity test, the catalyst (0.5 g), diluted with $\alpha\text{-}Al_2O_3$ (catalyst to diluent ratio 1:10 v/v), was loaded in the reactor and activated in situ at 270 °C and 0 barg for 1 h with syngas (H_2/CO = 2 mol/mol, GHSV = 6000 $cm^3(STP)/h/g_{cat}$). Then the reactor was cooled down to 220 °C and slowly pressurized until 30 barg. Process conditions were thus kept unchanged for 130 h until both the CO conversion rate and the product distribution reached a steady state. The study of CO_2 and CO reactivity was carried out by keeping constant both the H_2 partial pressure and the H/C ratio in the feed. To the scope, activity tests were performed in the presence of $H_2/CO_2/N_2$ (32/32/36 v/v), and $H_2/CO/N_2$ (32/32/36 v/v) mixtures (Table 2), keeping constant the other process conditions (T = 220 °C, P=30 barg, GHSV=6000 $cm^3(STP)/h/g_{cat}$). Tests with $H_2/CO/CO_2/Ar$ mixture were also carried out at the same process conditions, keeping P_{H_2}, P_{CO}, P_{CO_2} at the same levels used for the pure CO and CO_2 hydrogenation tests.

2.2.2. Co-based catalyst

$Co/\gamma\text{-}Al_2O_3$ catalyst was also tested in a lab-scale set-up operating 24/7 equipped with a stainless steel fixed bed reactor vertically inserted in an electric furnace. Additional information on the experimental rig and on the adopted process analytics are reported in Ref. [8].

Prior to the activity tests, the catalyst (3.0 g), diluted with $\alpha\text{-}Al_2O_3$ (1:2 v/v), was loaded in the reactor and reduced in situ at 400 °C and 0 barg for 16 h, feeding H_2 with a GHSV=4800 $cm^3(STP)/h/g_{cat}$. Then the reactor was cooled down to 180 °C, syngas was fed (H_2/CO = 2 mol/mol, GHSV = 4800 $cm^3(STP)/h/g_{cat}$), pressure was slowly increased until 20 barg and finally the reactor temperature was slowly increased to 220 °C. Process conditions were thus kept unchanged for about 130 h until both the CO conversion rate and the product distribution reached steady state values. Then the reactivity of the two following mixtures was investigated: H_2/CO (71.0/28.4 v/v), H_2/CO_2 (71.0/28.4 v/v). Ar (0.6 vol%) was used in all the experiments as internal standard for gas-chromatography (Table 3).

Table 4
Conversion and selectivity data measured during CO_2 and CO hydrogenation tests with Fe-based catalysts.

Sample tag	Fe2K			Fe4K			Fe10K		
Condition no.[a]	#1	#2	#3	#1	#2	# 3	#1	#2	# 3
CO conv. [%]	–	14.1	10.3	–	11.5	11.2	–	11.8	12.7
CO_2 conv. [%]	8.9	–	2.4	9.3	–	2.6	7.1	–	2.5
H_2 conv. [%]	16.1	21.4	24.9	19.9	22.2	30.3	18.4	25.6	33.0
CO sel. [%]	19.5	–	–	17.3	–	–	23.7	–	–
CO_2 sel. [%]	–	28.8	–	–	22.0	–	–	31.5	–

[a] Process conditions are given in Table 2.

3. Results

3.1. Fe-based catalyst

In this section, CO and CO_2 hydrogenation reactivity of our reference Fe-based catalyst, Fe4K sample, will be described. The role of potassium and its effects on the catalytic activity and selectivity will be discussed in Section 3.3.

Steady state CO_2, CO and H_2 conversion values measured in the test conditions #1 and #2 (Table 2) are reported in Table 4. During CO_2 hydrogenation (H_2/CO_2 = 1, condition #1) H_2 conversion was about 20%, while a CO_2 conversion value of about 9% was measured. Those conversion values, stable during the whole duration of the test (60–80 h), allowed to compute a H_2/CO_2 usage ratio of 2.1, which is lower than that given by the stoichiometry of the CO_2 hydrogenation to hydrocarbons (comprised among 3 and 4 depending on the product distribution, and expressed in the lumped form by Eq. (1)), because of the occurrence of the RWGS reaction (Eq. (2)).

$$nCO_2 + 3nH_2 \rightarrow (-CH_2-)_n + 2nH_2O \quad (1)$$

$$CO_2 + H_2 \leftrightarrow CO + H_2O \quad (2)$$

As a matter of facts, significant amounts of CO were detected in the products pool (CO selectivity >17%) (Table 4), along with water and gaseous and liquid hydrocarbons.

After the test in the presence of CO_2, the performances of the catalyst with H_2/CO mixtures (condition #2) were assessed for comparison purposes. In this condition, CO and H_2 conversions of 12% and 22% were measured, respectively, which are only slightly higher than those measured in the presence of the H_2/CO_2 mixture with the same H/C ratio. The corresponding H_2/CO usage ratio is 1.9, a value lower than that (comprised among 2 and 3 depending on the product distribution) predicted by the FT stoichiometry

Table 5
Conversion and selectivity data measured during CO and CO_2 hydrogenation tests with Co/γ-Al_2O_3 catalyst.

Condition number[a]	#1	#2
Condition tag	H_2/CO	H_2/CO_2
CO conversion [%]	22	–
CO_2 conversion [%]	–	33
H_2 conversion [%]	20	57
CO selectivity [%]	–	0
CO_2 selectivity [%]	<1	–

[a] Process conditions are given in Table 3.

(Eq. (3)) because of the occurrence of the WGS reaction (Eq. (4)) resulting in a CO_2 selectivity of 22%.

$$nCO + 2nH_2 \rightarrow (-CH_2-)_n + nH_2O \quad (3)$$

$$CO + H_2O \leftrightarrow CO_2 + H_2 \quad (4)$$

These results show that on the adopted iron based catalyst the activity of CO_2 is only slightly lower than that of CO at the same process conditions.

Interestingly, as opposite to CO_x conversion rates, the hydrocarbon distributions obtained from CO and CO_2 hydrogenations were found to be quite different (Fig. 1). In the case of CO (Fig. 1(b)) a straight Anderson-Schulz-Flory (ASF) distribution of hydrocarbon products was obtained, with a chain growth probability for the C_3–C_{10} species of 0.71 and a slight negative deviation from the linear trend for C_1 and C_2 species. Such result confirms the literature indications suggesting that iron based catalysts, especially when alkali-doped, are characterized by a low methane selectivity when used for CO hydrogenation [32]. In the case of CO_2 (Fig. 1(a)), on the contrary, the productivity of light hydrocarbons (C_1–C_3) is significantly higher and the chain growth probability for the C_3–C_{10} species decreases to a value of 0.65. This is in good agreement with the data reported in literature [9,13,14,19].

In Fig. 1(c) and (d) the fraction of olefins in C_2–C_{10} products is also shown as a function of the carbon number. Looking at Fig. 1(c), it is evident that CO_2 hydrogenation brings to saturated and unsaturated hydrocarbons with a fraction of olefins monotonically decreasing with the carbon number if one excludes C_2 species, which show a strong negative deviation from trend. The fraction of olefins in the products and their distribution as a function of the carbon number are different in the case of CO hydrogenation (Fig. 1(d)). In this case, indeed, the fraction of olefins is monotonically decreasing with the C number and tends to an asymptote value near 70% for C_4–C_{10} species.

Fig. 1(d) also shows that both the product distribution and the olefins content in the hydrocarbons are stable with time on stream (T.o.S.) during CO hydrogenations and a steady-state is quickly reached after switching back to the mixture H_2/CO after catalytic tests with CO_2 (Fig. 1(d), inset). On the contrary, during CO_2 hydrogenation, even if the ASF product distribution is rather stable with the T.o.S. (Fig. 1(a)), the fraction of olefins in the products progressively decreases (Fig. 1(c), inset). Such decreasing effect is more pronounced for the long-chain species, so that the curves in Fig. 1(c) became steeper with time-on-stream.

3.2. Co-based catalyst

At the adopted process conditions, also the un-promoted Co/γ-Al_2O_3 catalyst is active in the hydrogenation of both CO and CO_2 (Table 5). In this case, however, CO_2 conversion (33%) is higher than that of CO (22%) and requires an amount of hydrogen per mole of converted carbon that is almost three times higher than that used in the hydrogenation of CO. Accordingly, the H_2/CO_x usage ratio increases from a value very close to 2, measured in the case of CO hydrogenation and typical of a dominating FT regime (Eq. (3)), to a value slightly lower than 4, measured during CO_2 hydrogenation typical of CO_2 methanation (Eq. (5)) regime.

$$CO_2 + 4H_2 \rightarrow CH_4 + 2H_2O \quad (5)$$

Looking at reaction products (Table 5), very small amounts of CO_2 were measured during CO hydrogenation. Also, no CO was detected among the products in the case of CO_2 hydrogenation.

The ASF product distributions obtained during CO and CO_2 hydrogenations are reported in Fig. 2. During CO hydrogenation (Fig. 2(b)) a typical FT product distribution is obtained, characterized by a chain-growth probability 0.75 for the C_3–C_{10} species and methane and C_2 hydrocarbons out of trend. The product composition changes dramatically when the feed is switched to H_2/CO_2. In this case (Fig. 2(a)), as suggested by the H_2/CO_2 usage ratio, the main reaction product is methane (whose selectivity was more than 90%) and α is as low as 0.25.

The olefin contents in the hydrocarbons during CO and CO_2 hydrogenation are also shown in Fig. 2 as a function of the carbon number. The distribution obtained during CO hydrogenation (Fig. 2(d)), qualitatively very similar to that obtained on the Fe-based sample during the hydrogenation of CO_2 (Fig. 1(c)), is monotonically decreasing with increasing the carbon number (from 77% for propylene to 41% for C_{10} olefin), with ethylene showing a strong negative deviation from the trend (33%). In line with the results reported by Yao et al. [26], the olefin content in the products changes dramatically when the feed is switched from H_2/CO to H_2/CO_2: in the latter case (Fig. 2(c)) the only unsaturated molecules identified in the products are ethylene, propylene and butenes. Their fraction in the hydrocarbon is about 30%, a fairly low value, independent on the carbon number.

Notably, as opposite to Fe-based sample, the ASF distribution and the olefins content of hydrocarbons are very stable both during CO and CO_2 hydrogenation and quickly reach the steady state either when CO is replaced with CO_2 or vice-versa.

3.3. Effect of potassium loading

The results shown in previous section point out that iron based catalysts are more suitable than cobalt based catalysts to convert CO_2 in long-chain hydrocarbons. Considering this result, we have decided to further investigate the CO_2 hydrogenation on K-promoted Fe based catalysts. In particular, the effect on activity and selectivity of varying potassium loading was assessed by testing in CO_2 hydrogenation other two catalyst samples, whose K/Fe molar ratios were 0.02 (Fe2K) and 0.1 (Fe10K), respectively. The reactivity of CO/H_2 and CO/CO_2/H_2 mixtures was also comparatively investigated over these catalysts, so to verify if the co-presence of CO in the feed may affect CO_2 reactivity and vice versa.

3.3.1. CO_2 hydrogenation

As shown in Table 4, varying the potassium loading has only a slight effect on CO_2 conversion (condition #1). Minor effects have been also detected in terms of CO selectivity, which shows only a weak local minimum for the sample Fe4K, in correspondence to which a local maximum in the catalyst activity is observed. On the contrary, potassium has a strong effect on the composition of the hydrocarbon products, both in terms of average length chain growth probability (Fig. 3(a)) and in terms of olefin content in hydrocarbons pool (Fig. 3(b)). In particular, upon increasing the potassium loading, the chain growth probability grows from 0.56 to 0.64, as well as the olefins fraction in the C_2–C_{10} hydrocarbons. The increased C_{5+} selectivity and chain growth probability at high potassium loadings have been also reported in the literature [6,17,22,24].

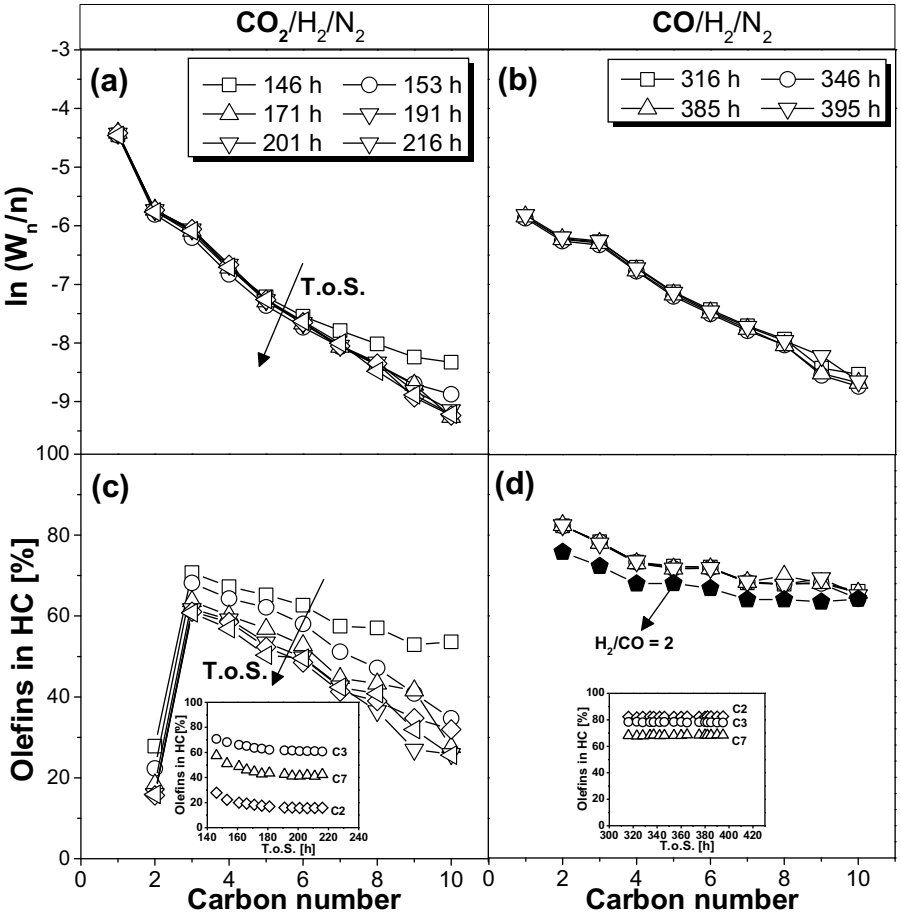

Fig. 1. Evolution with T.o.S. of: (a) ASF plots (shown in terms of productivity) and (c) fraction of olefins in hydrocarbon products as a function of the carbon number during CO_2 hydrogenation; (b) ASF plots and (d) fraction of olefins in hydrocarbon products as a function of the carbon number during CO hydrogenation. Data have been obtained with Fe4K catalyst at process conditions given in Table 2 (conditions #1 and #2).

Interestingly, upon changing the potassium loading, the "shape" of olefins distribution also changes, with the local maximum shifting from C_3 to C_4 when decreasing the K-loading.

Potassium also affects catalyst evolution with time-on-stream. Indeed, even though the olefins content of hydrocarbons decreases progressively with T.o.S. for all the tested samples, Fig. 4 shows that steady state conditions are achieved much faster for the samples with a high potassium loading.

3.3.2. CO/CO_2 hydrogenation

The effect of potassium loading was also investigated during the hydrogenation of CO and CO/CO_2 equimolar mixture. As shown in Table 4, the reactivity of Fe2K sample in the presence of CO and CO_2 (condition #3) is characterized by an average CO conversion rate which is about 30% slower than during pure CO hydrogenation (condition #2) and by an average CO_2 consumption rate which is more than 70% slower than in the absence of co-fed CO (condition #1). At the same time, both the product distribution and the olefin fraction in the products from CO/CO_2 hydrogenation (shown in Fig. 5) are very similar to those obtained during CO hydrogenation (Fig. 1(b) and Fig. 1(d), respectively). These data are in good agreement with a recent literature paper reporting that CO_2 behaves as inert at $CO_2/(CO+CO_2)$ ratios lower than 0.5–0.7 [14].

Interestingly, during CO/CO_2 hydrogenation, increasing the potassium loading has minor effects on the CO_2 conversion rate, while the CO conversion rate is slightly increased (Table 4). Besides, potassium loading has minor effect in terms of both chain growth probability and olefins content of the products (Fig. 5). The same trends are also observed during CO hydrogenation (data not shown).

Notably, the fact that higher potassium loadings boost α during CO_2 hydrogenation, while have minor effects on the chain growth probability during CO and CO/CO_2 hydrogenations, results in product distributions obtained during CO_2 and CO (or CO/CO_2) hydrogenations which show smaller differences at high K-loadings. This is in agreement with data by Herranz et al. [19], who have found that α decreases from 0.62 to 0.29 by switching from CO to CO_2 over an un-promoted Fe-Mn catalyst, whereas it decreases only from 0.62 to 0.56 for a 1.3 at.% K-promoted catalyst. Results bringing to the same conclusions have been also reported for highly promoted potassium Fe-catalyst [6,12].

4. Discussion

In this section, the different activity and selectivity of iron and cobalt FT catalysts in the presence of CO and CO_2 are discussed considering both the nature of the active sites, their coverage during CO and CO_2 hydrogenation and the differences in the dominant reaction pathways.

4.1. Comparison of the performances of Fe- and Co-based catalysts

4.1.1. Fe-based catalysts

Our results show that both CO and CO_2 are readily hydrogenated over iron based catalysts under low temperature Fischer-Tropsch

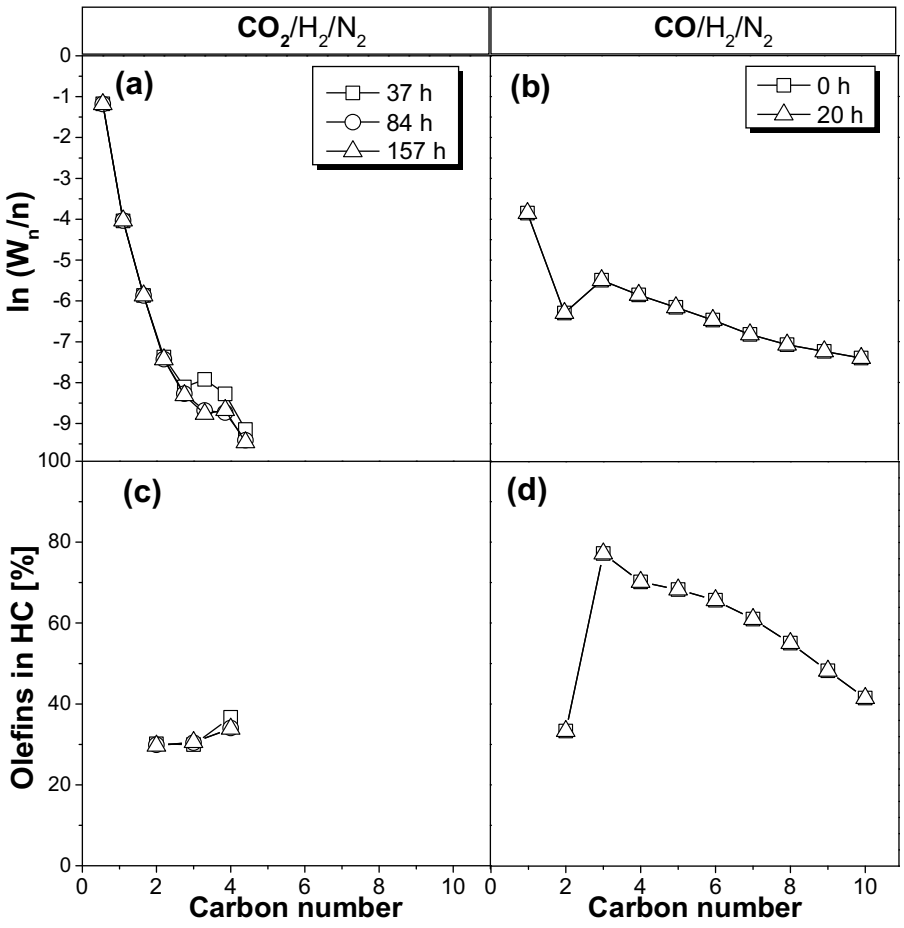

Fig. 2. Evolution with T.o.S. of: (a) ASF plots (shown in terms of productivity) and (c) fraction of olefins in hydrocarbon products as a function of the carbon number during CO_2 hydrogenation; (b) ASF plots and (d) fraction of olefins in hydrocarbon products as a function of the carbon number during CO hydrogenation. Data have been obtained with Co/γ-Al_2O_3 catalyst at process conditions given in Table 3.

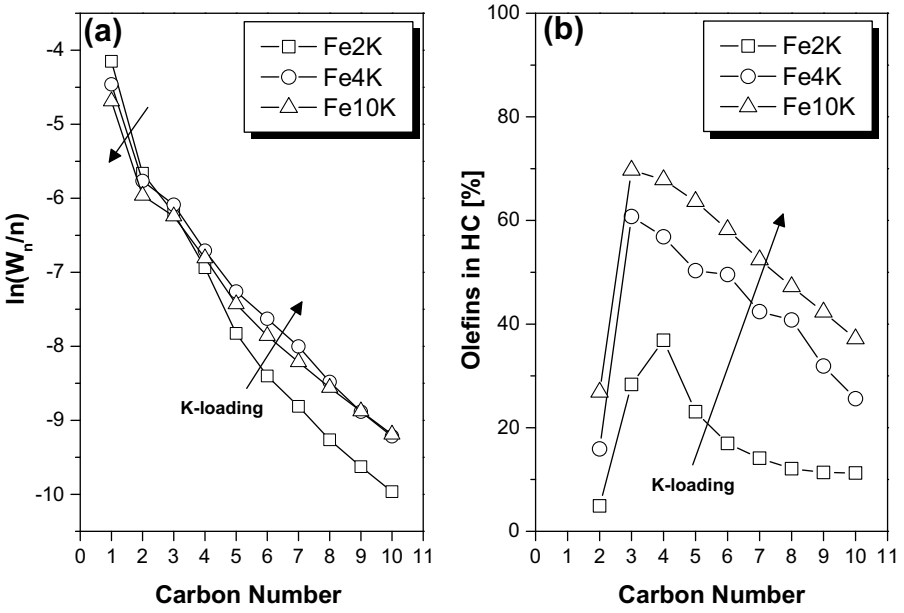

Fig. 3. (a) ASF plots and (b) fraction of olefins in hydrocarbon products as a function of the carbon number during CO_2 hydrogenation for Fe-based catalysts with different potassium loadings. Process conditions given in Table 2 (condition #1).

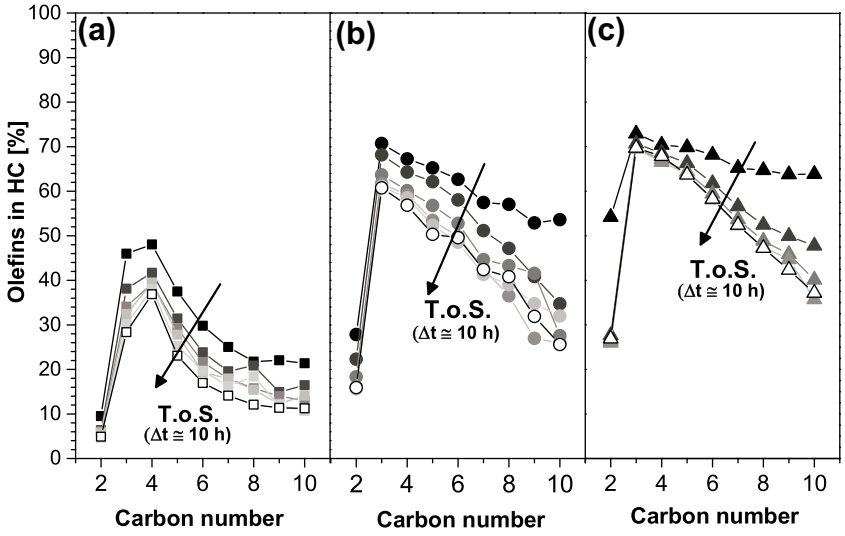

Fig. 4. Evolution with T.o.S. of olefin content in hydrocarbon products for (a) Fe2K, (b) Fe4K and (c) Fe10K catalysts used in CO_2 hydrogenation. Process conditions given in Table 2 (condition #1).

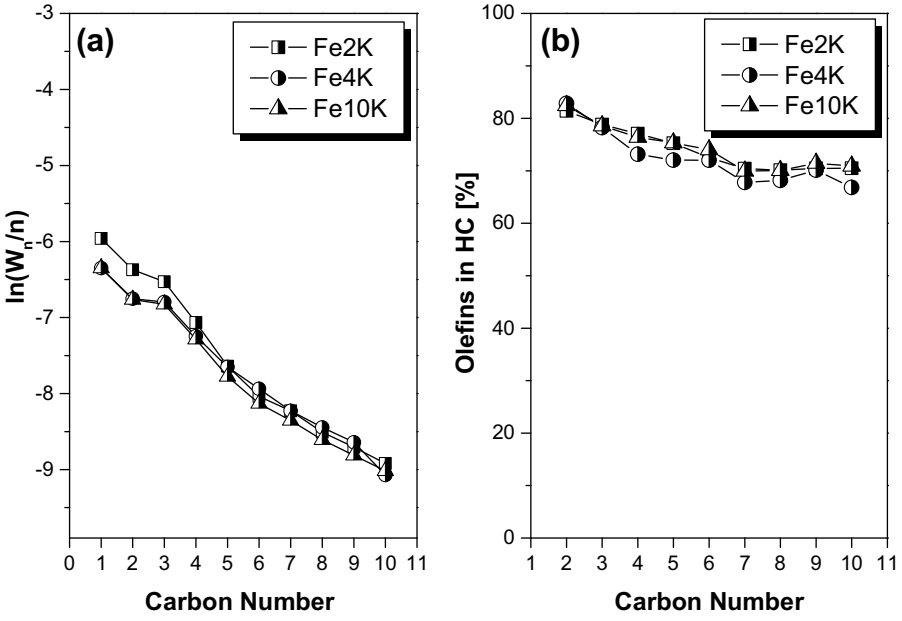

Fig. 5. (a) ASF plots and (b) fraction of olefins in hydrocarbon products as a function of the carbon number during the hydrogenation of $CO/H_2/CO_2$ mixture for Fe-based catalysts with different potassium loadings. Process conditions given in Table 2 (condition #3).

conditions, with CO_2 being only slightly less reactive than CO. Notably, Yao et al. [14] found that CO_2 hydrogenation rate on unpromoted Fe/TiO_2 catalyst is about 2.5 times slower than that of CO. A similar effect is also observed by other authors testing potassium promoted iron catalysts [9,12,19,22]. For example, working with a Fe-Al-Cu–25 K catalyst Riedel et al. [12] obtained conversions of 100% and 25% during CO and CO_2 hydrogenation, respectively. We speculate that the smaller difference between the hydrocarbon synthesis rates in the presence of CO and CO_2 observed with our catalyst is due to the low CO_x conversion values obtained under our conditions.

In spite of the similarity between CO and CO_2 conversion values, our results show that the product distributions obtained during CO and CO_2 hydrogenations are significantly different, with lighter and more saturated hydrocarbons produced when CO_2 replaces CO. This can be ascribed to two different phenomena. First of all, the different adsorption strength of CO_2 and CO on the catalyst surface (with CO_2 being less strongly adsorbed than CO) causes in the case of CO hydrogenation the increase of the chain growth probability (from 0.65 to 0.71) and the highest olefin fraction in the products. Indeed, the higher adsorption strength of CO results in a lower local H/C ratio [36] and this slows down the rates of hydrogenation reactions (including the secondary hydrogenation of α-olefins) favouring the chain growth process. Another reason for the lower content of olefins during CO_2 hydrogenation is that the lower CO partial pressure may boost the secondary reactions of olefins, whose kinetics are reported to be first order with respect to both 1-alkene and H_2, and negative order (between −1 and −2) with respect to CO, indicating a competitive adsorption process involving CO and the 1-alkene [37].

It is worth noticing that neither the difference in CO and CO_2 adsorption strengths nor the inhibition effect of CO on the secondary hydrogenation of olefins can explain the progressive decrease of the olefin fraction during CO_2 hydrogenation with

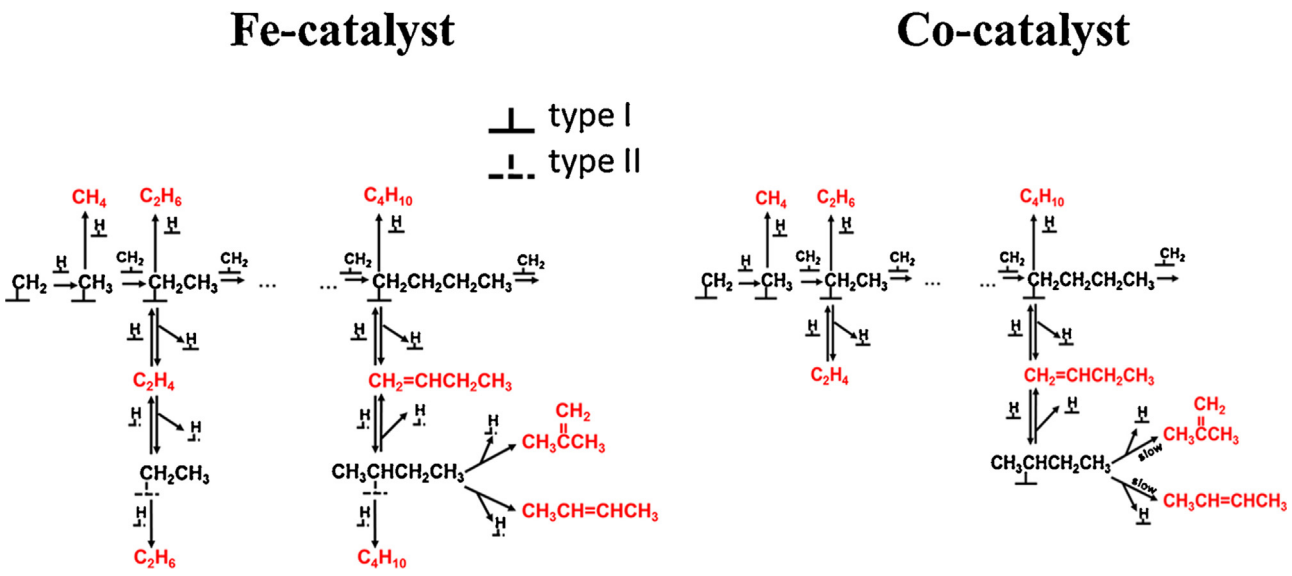

Fig. 6. Chain growth path for Fe-based and Co-based [8] catalysts during CO_2 and CO hydrogenation.

time-on-stream. In order to explain this behaviour, it can be speculated that two different catalytic sites exist on Fe-based catalyst: iron carbide centers (type I), which are responsible for the chain-growth process [12,21], and metallic iron or oxidized Fe-centers (type II) which are active sites for the secondary hydrogenation of olefins [38–40] (Fig. 6). The relative amount of chain growth and hydrogenation sites depends on the process conditions, since the hydrogenation sites can be transformed in chain growth sites through a carburization process at the expenses of CO, or site I can be transformed into site II through a decarburisation process involving CO_2 as oxidant.

As a matter of facts, in line with established literature indications [12], when the catalyst is treated in syngas ($H_2/CO = 2$) at high temperature (270 °C), iron oxides are transformed into iron carbides (possibly going through metallic iron centers), and hence a fraction of hydrogenation sites is transformed into growth sites. This explains why catalytic tests carried out with $H_2/CO = 2$ (Fig. 1(d)) are characterized by a high value of the chain growth probability and by a high olefin content in the products. The small residual amount of hydrogenation sites on the catalyst surface makes the secondary hydrogenation of olefins negligible and, as a result, the olefinic fraction of the products is substantially independent on the carbon number.

When CO_2 replaces CO in the feed, iron carbides are slowly reoxidized to Fe_3O_4 and amorphous FeO_x. This process is favoured by the high CO_2 and H_2O concentrations in the reactor [21]. As a result the number of hydrogenating sites increases and the olefin content in the products progressively decreases (as reported in Ref. [21]). Notably, the secondary hydrogenation of olefins is chain length dependent because, as already mentioned, the olefin diffusion rate in the catalyst pores depends on the chain length [38]. As a result, the slow diffusing olefins with high molecular weight undergo hydrogenation to the corresponding paraffins more easily than small olefins, and the distribution in Fig. 1(c) becomes steeper. Also, the higher is the number of hydrogenation sites, the steeper is the ASF product distribution (Fig. 1(a)) because the number of chain growth sites progressively decreases as a result of the catalyst decarburization. A new "equilibrium condition" is reached after a while, where the rate of carbides oxidation equilibrates the (slow) rate of carbides formation (possibly by CO in the products). This new equilibrium condition is characterized by a low olefinicity in the final product distribution.

This decarburization process, as well the carburization process, is (at least partially) reversible. Indeed, when we switched back to syngas ($H_2/CO = 1$) after CO_2 hydrogenation tests, the olefin secondary hydrogenations decreased, and the olefin content in the products grew back up to a higher steady value (Fig. 1(d)). We speculate that this is due to the fact that the equilibrium between iron carbides oxidation and iron carburization is shifted back to a higher carbides content, promoted by the high CO concentration in the gas phase. Interestingly, the dynamics of carbides reoxidation is slow as the products evolved for more than 70 h when switching from CO to CO_2. On the other hand, when we switched back to syngas ($H_2/CO = 1$) after CO_2 hydrogenation tests, the new steady state was rapidly reached, as shown in Fig. 1(d).

Notably, our results are different from those reported by Riedel et al. [12], who observed that the catalyst can be carburized both in the presence of CO and of CO_2, even though in this latter case the carburization process is much slower. Also, at variance with our data, Riedel et al. [12] observed that secondary hydrogenations of olefins occur only in an initial stage of the catalyst life, during which the catalyst undergoes a reconstruction which results in the disappearance of the olefins hydrogenation sites and in the formation of the chain growth ones. These differences can be explained by considering that the catalyst used by Riedel et al. [12] is strongly promoted with K (100Fe-13Al_2O_3-10Cu-25K atomic ratios), and has been tested in the presence of H_2/CO and H_2/CO_2 mixtures with molar ratios of 2 and 3, respectively, as dictated by the stoichiometries of reactions described by Eqs. (1) and (3). On the contrary, we worked with a much less K-promoted catalyst, and with H_2/CO and H_2/CO_2 mixtures having a molar H_2/C ratio of 1. Accordingly, in our conditions the oxidizing chemical potential is higher than in the experiments by Riedel et al. [12], and hence iron carbides on the surface are expected to be more easily converted to Fe oxides. In line with this explanation, using a Fe-catalyst with lower K/Fe ratios (<0.1 mol/mol), Gnanamani et al. [21] and Cubeiro et al. [23] found that during CO_2 hydrogenation the fraction of Fe_3O_4 and other oxidized Fe species (FeO_x) on the catalyst increases with the T.o.S. due to the oxidation of χ-Fe_5C_2 species.

4.1.2. Co-based catalysts

Our data show that the CO and CO_2 can be also effectively hydrogenated on a cobalt based catalyst. Contrary to iron catalyst, however, in this case CO_2 is more reactive than CO at the same process conditions and no CO is found in the product pool during CO_2

hydrogenation. These results are well aligned to those reported by Akin et al. [27] and Yao et al. [26]. It is well known that FT rate is negative order with respect to CO as consequence of the strong CO adsorption over cobalt sites [41,42], and that high CO partial pressure is required to establish FT regime. Co-based catalysts are not active in WGS/RWGS reactions [7], so during CO_2 hydrogenation the partial pressure of CO remains very low for establishing a FT regime and methane is the main product.

Looking at the product formation mechanism (Fig. 6), it is known that on cobalt-based catalysts chain growth occurs on the same sites where secondary hydrogenation of olefins also occurs [43]. These sites are usually identified as the reduced metal centers [41]. Since these metallic sites are responsible for both the chain growth and the olefin hydrogenation, as opposite to iron catalysts, the relative rate of the chain growth and secondary hydrogenation reactions cannot be independently tuned by modifying the nature of the active species under a dominating FT regime. Accordingly, we think that the different selectivities of CO and CO_2 hydrogenation processes are exclusively related to the different adsorption strengths of CO_2 and CO, which lead to very different H/C ratio on the surface. In particular, as reported in a number of papers [6,41], CO_2 adsorption on reduced cobalt centers is much weaker than CO adsorption. As a result, the local hydrogen fractional coverage during CO_2 hydrogenation is higher than during CO hydrogenation. This favours the chain termination reactions and thus shifts the process selectivity towards low molecular weight hydrocarbons, with a dominant paraffin content (Fig. 2). This is in line with the results of Schulz et al. [44], who have shown that the chain growth probability decreases upon increasing H_2 partial pressure and decreasing CO partial pressure.

The shift of the process selectivity is very strong, so that during CO_2 hydrogenation all the reaction products are in the gas phase at the adopted process conditions [45,46]. The absence of a liquid phase filling the catalyst pores makes the olefin pore diffusion faster, which results in a negligible probability for olefins to undergo secondary reactions. This is the reason why the olefin content in the hydrocarbons is low and independent on the carbon number.

4.2. Effect of potassium loading on Fe-based catalysts

4.2.1. CO_2 hydrogenation

Upon testing the Fe-based catalysts having different K loadings, we found that CO_2 conversion, as well as CO selectivity, varies only slightly. On the contrary, both the average molecular weight of the hydrocarbon products and their olefinicity increase upon increasing the potassium loading (Fig. 3).

These results can be explained by attributing to potassium a role in stabilizing/promoting the formation the carbides (type I sites) on the catalyst surface during CO_2 hydrogenation. In particular our results suggest that upon increasing the potassium content of the catalyst, more type I sites and less type II sites are available. As a consequence, the chain growth process is more effective (resulting in higher α values), and the secondary olefin hydrogenations decrease (resulting in higher olefin content).

In addition to this, the chain-growth probability increases with K-loading because the presence of potassium weakens H_2 chemisorption, thus making the catalyst less hydrogenating, that is more prone to make hydrocarbon chains growing, less active in H-additions to form paraffins, and more active in β-H-eliminations bringing to primary olefins.

Higher potassium loadings also increase the rate of formation of iron carbides starting from iron oxides. As a consequence, the higher is the K-content in the catalyst, the faster steady conditions are reached when CO_2 in the feed is replaced by CO and type II sites, more abundant during CO_2 hydrogenation, are replaced by type I sites, dominating the catalyst surface during CO hydrogenation. This explanation is in line with results by Fischer et al. [22], who have recently confirmed using an in-situ magnetometer that potassium has a promoting effect on the formation of χ-Fe_5C_2 (type I site) under reaction conditions.

Interestingly, upon changing the potassium loading, the olefin distribution also changes, with the local maximum that shifts from C_3 to C_4 when decreasing the K-loading, and the slope of the C_{4+} distribution which becomes steeper (Fig. 4). This behaviour can be explained by considering that among the C_{4+} olefins terminal and internal species are formed: Fe-based catalysts, indeed, activate the double-bond-shift reactions on type II sites [47]. Internal olefins, which are secondary products, are less reactive than terminal ones (primary products), and consequently are less prone to be hydrogenated and to be involved in secondary reactions. This preserves the content of C_{4+} olefins in the product pool.

Our data, in line with [47], point out that the lower is the potassium loading, i.e. the higher is the concentration of type II sites, the higher is the double bond shift activity (Fig. 6). As a matter of facts, the content of the internal isomer within C_4 olefins is 46.4% for Fe2K, 12.2% for Fe4K and 11.4% for Fe10K.

Notably, the double bond shift mechanism is not effective in preserving ethylene and propylene, which do not have internal isomers. In line with this, our data show that catalysts with a high concentration of type II sites bring to products with very low C_2 and C_3 olefins (Fig. 4). Also, in the case of the Fe2K catalyst, the amount of propylene which is found in the products is smaller than the amount of butenes. This is due to the fact that while butenes are partially stabilized by the double bound shift, propylene is not.

The smooth slope of the curves shown in Fig. 4(a) for Fe2K sample is an additional proof that the double-bond shift extensively occurs on this catalytic system.

4.2.2. CO_2/CO hydrogenation

Upon testing the Fe-based catalysts having different K loadings in the presence of $CO/H_2/CO_2$ mixtures we observed that, regardless the K-content of the catalyst, CO_2 co-fed with CO is converted with a rate smaller than in the absence of CO. This can be explained by considering that a competitive adsorption exists between CO and CO_2, in which CO largely prevails.

Nevertheless even though the CO_2 conversion rate is strongly decreased in the presence of CO, our data show that the cofeeding of CO_2 to CO/H_2 mixtures (at constant H/C ratio) can be used to prevent that a part of carbon contained in converted CO is transformed into undesired CO_2. Indeed, the presence of CO_2 in the feed does not affect significantly CO conversion, but makes nil the net production of CO_2. Accordingly this is a way to increase the atom efficiency of the CO conversion process.

Interestingly, the catalyst activity is stable in the presence of CO/CO_2 mixtures. This suggests that the stability of iron carbides, which is partially compromised during pure CO_2 hydrogenation tests, is now preserved by the high CO partial pressures.

As opposite to CO_2 hydrogenation, during CO or CO/CO_2 hydrogenations α-olefins dominate the products, as demonstrated for example by the fact that 1-butene represents over 90% of C_4 olefins. This suggests that the secondary reactions of the olefins are negligible in the presence of CO. Again, such results can be explained considering that the presence of stable iron carbides during CO and CO/CO_2 hydrogenation tests does not allow the formation of sites active in secondary reactions. This is in line with literature indications according to which the primary selectivity to olefins and the presence of hydrogenating sites depend only slightly from the reaction temperature and pressure [48], but are strongly affected by the catalyst activation procedure and feed composition.

During the hydrogenation of CO_2/CO mixtures, the potassium loading has only minor effects. Indeed, CO conversion is only

slightly promoted by the addition of more potassium, while CO_2 conversion is substantially unaffected and remains very low. In this case, potassium has weak effects also on the product distribution, as shown for example in Fig. 5 for what concerns the ASF product distribution and the olefin content in the hydrocarbon product pool.

Following these evidences our results point out that, as opposite to the case of CO_2 hydrogenation, during the hydrogenation of CO/CO_2 mixtures the potassium loading on the catalyst does not need to be high in order to promote the chain growth probability. Indeed, in the presence of co-fed CO, the concentration of atomic oxygen adsorbed on the surface is kept intrinsically low by the strong CO adsorption. This limits the formation of type II sites and eventually prevents the olefins secondary reactions to happen.

5. Conclusions

By comparing the reactivity of cobalt and iron Fischer-Tropsch catalysts during CO, CO_2 and CO/CO_2 hydrogenation processes, key-differences and peculiarities are observed.

On cobalt based catalysts, CO_2 is more reactive than CO, but brings to completely different products: the methanation regime dominates in the presence of CO_2/H_2 mixtures, while the FT regime dominates in the presence of syngas. On K-promoted iron based catalysts, on the contrary, CO_2 is slightly less reactive than CO, but the hydrogenation of both CO and CO_2 occurs under a Fischer-Tropsch controlled regime accompanied by a WGS or a RWGS regime. The products from CO hydrogenation are dominated by waxes, while those from CO_2 contain mainly middle distillates. Also, more saturated species are found in the hydrocarbons pool when carrying out the CO_2 hydrogenation.

Our data suggest that, on both cobalt and iron based catalysts, CO and CO_2 hydrogenation processes follow a common reaction pathway, with CO acting as intermediate (quickly converted on Co-based catalysts) in the case of CO_2 conversion. The different selectivity of the two processes, however, is due to several reasons. On cobalt-based catalyst it has to be ascribed to different H/C ratio that is attained on the catalyst surface due to the different adsorption strengths of CO and CO_2. On iron-based catalysts this is still occurring, but the dominant phenomenon controlling the process selectivity is the equilibrium between the chain growth sites (iron carbides), which are stable only in the presence of high CO partial pressures, and the hydrogenation sites (iron oxides and reduced iron centers), which are formed when CO is removed from the feed and which are active in the secondary reactions of olefins. The relative abundance of these two types of sites is affecting conversion and selectivity.

Finally, we have studied the effect of K-loading on the activity and on the selectivity of the adopted iron-based catalyst. We have found that this promoter has a minor effect on the CO and CO_2 hydrogenation activity, but it dramatically changes the selectivity in the presence of CO_2. High K-loadings were found able to promote the chain growth process and the formation of primary olefins. These results can be explained on the basis of the effects of K-promotion on (i) the stability of the iron carbide species; (ii) the inhibition of the double-bond shift, and (iii) the electronic properties of Fe, which result in modified adsorption strengths of H_2, CO and CO_2.

The reactivity of cobalt and iron-based FT catalysts in CO_2 hydrogenation and the possibility of obtaining methane or middle distillates open new perspective in view of CO_2 reutilization and valorisation, in addition to well know processes like CO_2 methanation over Ru and Ni catalysts and CO_2 conversion to methanol and its derivatives.

References

[1] X. Xiaoding, J.A. Moulijn, Energy Fuels 10 (1996) 305–325.
[2] W. Wang, S. Wang, X. Ma, J. Chem. Soc. Rev. 40 (2011) 3703–3727.
[3] K. Stephenne, Energy Procedia 63 (2014) 6106–6110.
[4] K.M.K. Yu, I. Curcic, J. Gabriel, S.C.E. Tsang, ChemSusChem 1 (2008) 893–899.
[5] P. Kaiser, R.B. Unde, C. Kern, A. Jess, Chem. Ing. Tech. 85 (2013) 489–499.
[6] M.K. Gnanamani, G. Jacobs, W.D. Shafer, D. Sparks, B.H. Davis, Catal. Lett. 141 (2011) 1420–1428.
[7] T. Riedel, M. Claeys, H. Schulz, G. Schaub, S.S. Nam, K.W. Jun, M.J. Choi, G. Kishan, K.W. Lee, Appl. Catal. A: Gen. 186 (1999) 201–213.
[8] C.G. Visconti, L. Lietti, E. Tronconi, P. Forzatti, R. Zennaro, E. Finocchio, Appl. Catal. A: Gen. 355 (2009) 61–68.
[9] M.K. Gnanamani, W.D. Shafer, D.E. Sparks, B.H. Davis, Catal. Commun. 12 (2011) 936–939.
[10] Y. Zhang, G. Jacobs, D.E. Sparks, M.E. Dry, B.H. Davis, Catal. Today 71 (2002) 411–418.
[11] G.D. Weatherbee, C.H. Bartholomew, J. Catal. 87 (1984) 352–362.
[12] T. Riedel, H. Schulz, G. Schaub, K.W. Jun, J. Hwang, K.W. Lee, Top. Catal. 26 (2003) 41–54.
[13] H. Ando, Y. Matsumura, Y. Souma, J. Mol. Catal. A: Chem. 154 (2000) 23–29.
[14] Y. Yao, X. Liu, D. Hildebrandt, D. Glasser, Ind. Eng. Chem. Res. 50 (2011) 11002–11012.
[15] Y. Liu, C.H. Zhang, Y. Wang, Y. Li, X. Hao, L. Bai, H.W. Xiang, Y.Y. Xu, B. Zhong, Y.W. Li, Fuel Process. Technol. 89 (2008) 234–241.
[16] T. Riedel, G. Schaub, K.W. Jun, K.W. Lee, Ind. Eng. Chem. Res 40 (2001) 1355–1363.
[17] R.W. Dorner, D.R. Hardy, F.W. Williams, H.D. Willauer, Appl. Catal. A: Gen. 373 (2010) 112–121.
[18] R.A. Fiato, E. Iglesia, G.W. Rice, Stud. Surf. Sci. Catal. 114 (1998) 339–344.
[19] T. Herranz, S. Rojas, F.J. Pérez-Alonso, M. Ojeda, P. Terreros, J.L.G. Fierro, Appl. Catal. A: Gen. 311 (2006) 66–75.
[20] M. Martinelli, C.G. Visconti, L. Lietti, P. Forzatti, C. Bassano, P. Deiana, Catal. Today 228 (2014) 77–88.
[21] M.K. Gnanamani, G. Jacobs, H.H. Hamdeh, W.D. Shafer, B.H. Davis, Catal. Today 207 (2013) 50–56.
[22] N. Fischer, R. Henkel, B. Hettel, M. Iglesias, G. Schaub, M. Claeys, Catal. Lett. 146 (2016) 509–517.
[23] M.L. Cubeiro, H. Morales, M.R. Goldwasser, M.J. Perez-Zurita, F. Gonzàlez-Jimènez, C.U. de N, Appl. Catal. A: Gen 189 (1999) 87–97.
[24] P.S.S. Prasad, J.W. Bae, K.-W. Jun, K.-W. Lee, Catal. Surv. Asia 12 (2008) 170–183.
[25] Y. Yao, X. Liu, D. Hildebrandt, D. Glasser, Appl. Catal. A: Gen 433–434 (2012) 58–68.
[26] Y. Yao, X. Liu, D. Hildebrandt, D. Glasser, Chem. Eng. J. 193–194 (2012) 318–327.
[27] A.N. Akin, M. Ataman, A.E. Aksoylu, Z.I. Onsana, React. Kinet. Catal. Lett. 76 (2002) 265–270.
[28] J.A. Dìaz, A.R. de la Osa, P. Sànchez, A. Romero, J.L. Valverde, Catal. Commun. 44 (2014) 57–61.
[29] G. Melaet, A.E. Lindeman, G. Somorjai, Top. Catal. 57 (2014) 500–507.
[30] G.P. Van der Laan, A.A.C.M. Beenackers, Catal. Rev. Sci. Eng. 41 (1999) 255–318.
[31] D.H. Chun, H.T. Lee, J.I. Yang, H.J. Kim, J.H. Yang, J.C. Park, B.K. Kim, H. Jung, Catal. Lett. 142 (2012) 452–459.
[32] S. Li, A. Li, S. Krishnamoorthy, E. Iglesia, Catal. Lett. 77 (2001) 197–205.
[33] D.B. Bukur, D. Mukesh, S.A. Pate, Ind. Eng. Chem. Res. 29 (1990) 194–204.
[34] D.G. Miller, M. Moskovits, J. Phys. Chem. 92 (1988) 6081–6085.
[35] H. Arakawa, A.T. Bell, Ind. Eng. Chem. Process Des. Dev. 22 (1982) 97–103.
[36] C.G. Visconti, E. Tronconi, L. Lietti, P. Forzatti, S. Rossini, R. Zennaro, Top. Catal. 54 (2011) 786–800.
[37] G. Sudheimer, J. Gaube, Ger. Chem. Eng. 8 (1985) 195–202.
[38] H. Schulz, Catal. Today 228 (2014) 113–122.
[39] M.E. Dry, T. Shingles, L.J. Boshoff, G.J. Oosthuizen, J. Catal. 199 (1969) 190–199.
[40] H. Schulz, H. Gokcebay, Catalysis of Organic Reaction, in: J.R. Kosak (Ed.), Marcel Dekker, New-York, 1984, pp. 153–169.
[41] C.G. Visconti, E. Tronconi, L. Lietti, R. Zennaro, Chem. Eng. Sci. 62 (2007) 5338–5343.
[42] L. Fratalocchi, C.G. Visconti, L. Lietti, E. Tronconi, S. Rossini, Appl. Catal. A: Gen. 512 (2016) 36–42.
[43] F. Fiore, L. Lietti, G. Pederzani, E. Tronconi, R. Zennaro, P. Forzatti, in: X. Bao, Y. Xu (Eds.), Natural Gas Conversion VII 2004, Stud. Surf. Sci Catal. 147, Elsevier Amsterdam (2004) 289–294.
[44] H. Schulz, E. van Steen, M. Claeys, Stud. Surf. Sci. Catal. 81 (1994) 455–460.
[45] C.G. Visconti, M. Mascellaro, Catal. Today 241 (2013) 61–73.
[46] C.G. Visconti, Ind. Eng. Chem. Res. 53 (2014) 1727–1734.
[47] H. Schulz, G. Schaub, M. Claeys, T. Riedel, Appl. Catal. A: Gen. 186 (1999) 215–227.
[48] H. Schulz, E. Van Steen, M. Claeys, Top. Catal (1995) 223–234.